PATHOGENS AND GLOBAL HEALTH
2024, VOL. 118, NO. 5, 429–449
https://doi.org/10.1080/20477724.2023.2240085

Taylor & Francis
Taylor & Francis Group

RESEARCH ARTICLE

Stem cell-derived exosomes as a potential therapy for schistosomal hepatic fibrosis in experimental animals

Asmaa R. Ellakany[a], Hanan El Baz[b], Zeinab S. Shoheib[a], Mohamed Elzallat[b], Dalia S. Ashour[a] and Nabila A. Yassen[a]

[a]Medical Parasitology Department, Faculty of Medicine, Tanta University, Tanta, Egypt; [b]Immunology Department, Theodor Bilharz Research Institute, Cairo, Egypt

ABSTRACT

Schistosomiasis is a neglected tropical disease. Egg-induced granuloma formation and tissue fibrosis are the main causes of the high morbidity and mortality of schistosomiasis. Mesenchymal stem cells (MSCs)-derived exosomes play an important role with a superior safety profile than MSCs in the treatment of liver fibrosis. Therefore, the aim of this study was to investigate the potential therapeutic effect of MSCs-derived exosomes on schistosomal hepatic fibrosis. Exosomes were isolated from bone marrow MSCs and characterized. A total of 85 mice were divided into four groups: group I (control group), group II (PZQ group) infected and treated with PZQ, group III (EXO group) infected and treated with MSCs-derived exosomes and group IV (PZQ+EXO group) infected and treated with both PZQ and MSCs-derived exosomes. Assessment of treatment efficacy was evaluated by histopathological and immunohistochemical examination of liver sections by proliferating cell nuclear antigen (PCNA) and nuclear factor-κB (NF-κB). The results showed significant reduction of the number and diameter of hepatic granulomas, hepatic fibrosis, upregulation of PCNA expression and reduction of NF-κB expression in EXO and PZQ+EXO groups as compared to other groups at all durations post infection. Additionally, more improvement was observed in PZQ+EXO group. In conclusion, MSCs-derived exosomes are a promising agent for the treatment of schistosomal hepatic fibrosis, and their combination with PZQ shows a synergistic action including antifibrotic and anti-inflammatory effects. However, further studies are required to establish their functional components and their mechanisms of action.

KEYWORDS

Schistosomiasis; stem cell-derived exosomes; liver fibrosis; NF-κB; PCNA; beads-based flow cytometry

Introduction

Schistosomiasis is a helminthic infection with a significant public health problem in many developing countries [1]. Furthermore, it is an endemic disease that affects approximately 240 million people worldwide [2]. Chronic schistosomiasis is caused by egg deposition, which results in chronic hepatosplenic schistosomiasis with granuloma formation and periportal fibrosis leading to portal hypertension [3,4].

Currently, the treatment of schistosomiasis continues to depend on praziquantel (PZQ) [5]. However, PZQ cannot resolve the progression of chronic hepatic fibrosis completely [6]. It is noteworthy that no efficacious therapeutic options for schistosomiasis-induced liver fibrosis are available till now. Therefore, there is an urgent need to develop therapeutic methods for preventing and/or treating liver fibrosis [7].

Mesenchymal stem cells (MSCs) therapy has developed as an emerging alternative method for treating many diseases including liver fibrosis [8]. Previous researches have revealed that bone marrow MSCs (BM-MSCs) could improve schistosomal hepatic fibrosis [9,10]. However, there are several safety issues related to MSCs-based therapy such as infusional toxicities, rejection of cells by the host, possible malignant transformation and ectopic tissue formation. Moreover, one of the major limitations is the difficulty of producing a consistent source of cells with a stable phenotype [11,12].

Exosomes are nano-sized MSCs-sourced extracellular vesicles which are released into the extracellular milieu [13]. Recent studies have shown that the therapeutic effect of MSCs is largely mediated by exosomes [14]. Currently, it is suggested that MSCs-derived exosomes are a good substitute for the biological MSCs activity [15].

MSCs-derived exosomes are involved in immunomodulatory activities and cell communication [16]. Also, they are involved in inhibition of fibrosis, stimulation of extracellular matrix remodeling and tissue repair, abrogation of local inflammation response and immune cells activities regulation [14,17].

Utilizing MSCs-derived exosomes as a therapy has numerous advantages compared to using MSCs themselves [18]. They are a cell-free therapy which would reduce safety issues about injecting live cells [19]. Besides, exosomes can cross the barriers such as

CONTACT Asmaa R. Ellakany asmaa.rashad@med.tanta.edu.eg; arashad20@yahoo.com Medical Parasitology Department, Faculty of Medicine, Tanta University, Tanta 31527, Egypt

blood–brain barriers and capillaries, and their size is small enough to evade the reticuloendothelial system [20]. Other features of MSCs-derived exosomes are no tumorigenic risk and high stability cell- and tissue-specific homing [21]. Consequently, MSCs-derived exosomes could represent a promising therapeutic strategy alternative to cell-based therapy for various diseases [22].

The administration of MSCs-derived exosomes has the ability to treat hepatic diseases such as liver fibrosis and injury by the delivery of various bioactive molecules to hepatocytes and other cells in the liver tissue [23]. Accordingly, the current work aimed to investigate the potential therapeutic and antifibrotic effects of MSCs-derived exosomes, given at different durations post infection (P.I.) with *Schistosoma mansoni* (*S. mansoni*) in a murine model.

Materials and methods

Culture and isolation of stem cells

Swiss albino rats were used to isolate BM-MSCs from bone marrow of the femurs and tibiae according to Ahmad and Shakoori [24]. Briefly, the epiphyses of femurs and tibiae were cut, and the bone marrow was flushed out using 5 mL of Dulbecco's modified Eagle's medium (DMEM). The cell mixture was suspended in 10 mL of complete medium (DMEM containing glutamine, 10% FBS, 100 U/mL penicillin and 100 µg/mL streptomycin). The cells were initially seeded into 6-well plate using a complete DMEM and incubated in a CO_2 incubator at 37°C in an atmosphere of 90% relative humidity and 5% CO_2. The first medium change was done 2 weeks after seeding, and then the medium was changed twice weekly. The cells were incubated until cells adhered and looked nearly confluent. When the cells reached 90–95% confluency, they were detached with 0.25% trypsin at 37°C for 7 min. Viability count was performed by mixing equal volumes of cell suspension and trypan blue.

According to Gang et al. [25], cells from the 3rd and 4th passages were washed twice in phosphate-buffered saline (PBS) buffer supplemented with 0.5% FBS by centrifugation at 2200 rpm for 5 min at 20°C then suspended at a concentration of 3×10^6 cells in 1 ml PBS. According to manufacturer's instructions, fluorescein isothiocyanate (FITC) rat anti-mouse CD90, CD44, CD31 and CD45 (BD Biosciences, San Jose, CA, U.S.A.) were added to flow cytometry tubes. Then, 100 µl sample was added to each tube, mixed well and incubated for 20 min at 4°C. Negative control was prepared by the addition of 100 µl of sample to an empty flow cytometry tube. The final analysis was done using the flow cytometer (Beckman Coulter, U.S.A.).

Isolation and characterization of exosomes

Isolation of exosomes

BM-MSCs-derived exosomes were isolated by differential ultracentrifugation according to Théry et al. [26]. Briefly, the culture medium was collected and centrifuged at 4°C for 300×g for 10 min then 2000×g for 10 min, and the precipitate was removed to remove cell fragments. Then, the supernatant was centrifuged at 10,000×g for 30 min to remove the subcellular components, then ultracentrifuged at 100,000×g for 70 min to form the final sediment, which contains the exosomes. The pellet was collected and washed in 50 ml PBS and then centrifuged again at 100,000×g for 70 min. The precipitate was suspended in PBS, and the samples were stored at −80°C until use.

Characterization of exosomes

Total protein amount: the total protein content in the samples was measured in triplicate using Qubit protein assay kit and Qubit 2 Fluorometer (Invitrogen, Thermo Scientific, U.S.A.), and the reported result was the average of the three readings.

Sodium dodecyl sulfate-polyacrylamide gel electrophoresis (SDS-PAGE): the exosomal proteins were separated by SDS-PAGE through a porous acrylamide gel matrix that separated proteins on the basis of their molecular weight. The gel was stained with Coomassie blue for analysis [27].

Scanning electron microscopy (SEM): the isolated BM-MSCs-derived exosomes were characterized by SEM according to Sokolova et al. [28]. The samples were fixed with 3.7% glutaraldehyde in PBS for 15 min. After washing twice with PBS, the samples were dehydrated with serial dilutions of ethanol. After evaporation of ethanol, they were left to dry at room temperature, then mounted on aluminum microscopy stubs and coated with gold (Au) for 30s using sputter coater (Q150T; Quorum Technologies Ltd, England). Scanning electron microscopic analysis was made using Tescan SEM (Tescan Vega 3 SBU, the Czech Republic).

Dynamic light scattering: it was used for determination of particle size. This was conducted using a 90Plus Brookhaven zetasizer (Brookhaven Instrument Corp., Holtsville, NY, U.S.A.). Sample preparation involved dilution of vesicles (1 in 200) using pre-filtered distilled water. Size measurement was conducted at a fixed angle (90°) at 25°C. The mean diameter value was recorded after data analysis using the system software [29].

Beads-based flow cytometry for exosomes surface markers: exosomes were identified by beads-based flow cytometry assessing the presence of tetraspanins (CD63), glycosylphosphatidylinositol (GPI)-anchored 5′nucleotidase (CD73) and thymus cell antigen 1 (CD90) [30]. Flow cytometric analysis of exosomes

was carried out according to Suárez et al. [31]. In brief, 50 µl of exosomes was reacted with 0.25 µl aldehyde/sulfate beads for 15 min at room temperature. Then, 1 ml PBS supplemented with 0.1% bovine serum albumin was added, and the sample was incubated overnight on rotation. Bead-coupled exosomes were centrifuged at 2000×g for 10 min, the pellet was washed and centrifuged again. Then, 50 µl buffer was added to the pellet and stained using anti-CD63, anti-CD73 and anti-CD90 as primary antibodies and FITC-conjugated secondary antibodies for 30 min at 4°C. Results were obtained using the NovoCyte flow cytometer (ACEA Biosciences Inc.) and NovoExpress software. Isotype control antibodies were used as a negative staining control. Each measurement was performed in technical triplicates.

Animals and experimental infection

This study was carried out on 85 laboratory-bred parasite-free male Swiss albino mice 6 weeks old and 20–25 gm weight obtained from Theodore-Bilharz Research Institute (Giza, Egypt). In accordance with the national and institutional guidelines, all mice were allowed to adapt for 4 days before they were included in the study with rodent chow and water ad libitum. Additionally, five Swiss albino rats were used as donors of BM-MSCs.

Laboratory-bred infected *Biomphalaria alexandrina* snails were exposed to light for at least 4 h for cercarial shedding. Mice were infected subcutaneously with *S. mansoni* cercariae shed from the snails '60 ± 10 cercariae/animal' as described by Holanda and colleagues [32].

Therapeutic agents

Praziquantel: it was available as Distocide (EIPICO) 600 mg tablets. The drug was administered orally in a dose of 500 mg/kg body weight/mouse for two consecutive days [33].

MSCs-derived exosomes: each mouse was treated with exosomes derived from 2×10^6 MSCs by intraperitoneal injection.

Experimental design and sampling

Mice were divided into four groups: group I (infected control group, 20 mice) *S. mansoni*-infected non-treated mice (positive control), group II (PZQ group, 20 mice) *S. mansoni*-infected mice that received PZQ at the 6th week P.I., group III (EXO group, 20 mice) was subdivided into two subgroups; subgroup IIIa *S. mansoni*-infected mice received MSCs-derived exosomes at the 6th week P.I. and subgroup IIIb *S. mansoni*-infected mice received MSCs-derived exosomes at the 10th week P.I. and group IV (PZQ+EXO group, 20 mice) was subdivided into two subgroups; subgroup IVa *S. mansoni*-infected mice received both PZQ and MSCs-derived exosomes at the 6th week P.I. and subgroup IVb *S. mansoni*-infected mice received PZQ at the 6th week P.I. and MSCs-derived exosomes at the 10th week P.I. Another five non-infected non-treated mice were used as negative control (Figure 1).

Early treatment at 6 weeks P.I. was chosen to investigate the anti-inflammatory effect of exosomes on restoring the liver condition when the granuloma is still cellular and late treatment at 10 weeks P.I. was chosen to ensure the occurrence of schistosomal hepatic fibrosis in order to investigate the antifibrotic effect of exosomes on the well-formed fibrotic granulomas.

Control infected mice (GI) and PZQ-treated group (GII) were sacrificed at 8, 10, 12 and 14 weeks P.I. while infected mice that were treated with exosomes at 6 weeks P.I. (GIIIa & GIVa) were sacrificed at 8 and 10 weeks P.I. and those treated at 10 weeks P.I. (GIIIb & GIVb) were sacrificed at 12 and 14 weeks P.I. (5 mice from each infected group at each duration). Control non-infected mice were sacrificed at the end of the experiment. Blood samples were collected for sera preparation, and the sera were kept at −20°C until used. Liver was removed and preserved in 10%

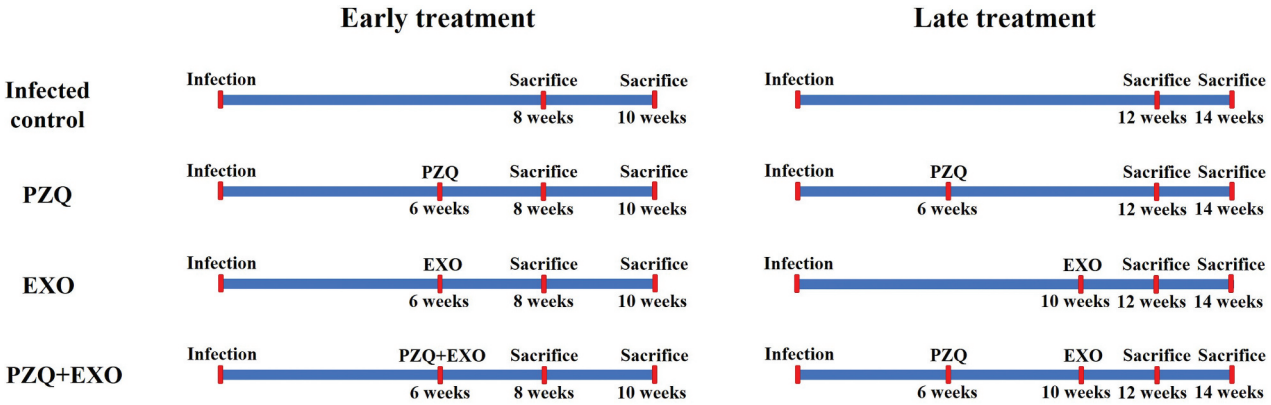

Figure 1. Experimental design. Mice received early treatment with exosomes at 6 weeks P.I. were sacrificed at 8 and 10 weeks P.I. and those received late treatment with exosomes at 10 weeks P.I. were sacrificed at 12 and 14 weeks P.I.

formalin for histopathological and immunohistochemical studies.

Evaluation of therapy

Histopathological examination of the liver

Estimation of the number and diameter of hepatic granulomas: paraffin blocks were prepared from the livers, and serial sections (5 µm) were cut from each specimen and stained with hematoxylin and eosin (H&E) [34]. For each mouse, the number of granulomas was determined in 10 fields (×100), then the mean number of granulomas/liver section was calculated and the composition was assessed. The largest diameter of the liver granuloma was measured using image analysis software Fiji (http://fiji.sc), and then the mean diameter of granulomas/liver section was calculated.

Morphometric assessment of liver fibrosis: Masson's trichrome staining was done to analyze the extent of liver fibrosis and to observe collagen fiber deposition. Collagen is shown as blue discoloration. The hepatic deposition of collagen was quantified by the percentage area of fibrosis stained with blue color using image analysis software Fiji [35].

Immunohistochemical examination of the liver

Immunohistochemical staining of liver sections using the primary antibodies: proliferating cell nuclear antigen (PCNA) to assess the regenerative effect of exosomes and nuclear factor-κB (NF-κB) to assess the inflammatory reaction. Immunoreactivity of PCNA sections was shown as brown staining of nuclei [36]. Their staining intensity was evaluated quantitatively as low and high expression. While immunoreactivity of NF-κB appeared as brown cytoplasmic or nuclear staining of varying degrees of intensity, it was evaluated quantitatively as weak, moderate and strong [37].

For the quantitative estimation of the number of positive cells, morphometric analysis was performed on immunostained sections. Quantification of PCNA and NF-κB expression was performed by selecting three random areas at 400× from each slide. Those areas were captured for image analysis. The number of positive cells/field was counted using the plug-in 'cell counter' in the image analysis software, and the mean number was calculated.

Ethics statement

The study protocol was approved and conducted according to the guidelines of the Laboratory Animal Centre for Research Ethics Committee, Faculty of Medicine, Tanta University (Approval number 34,128/9/20).

Statistical analysis

Data were presented as means ± standard deviation (SD). Analysis of variance (ANOVA) with post hoc Tukey test was used to determine the significance of differences between groups. Differences were considered not significant when ($P > 0.05$) and statistically significant when ($P < 0.05$). The statistical analyses were processed according to the conventional procedures using Statistical Program of Social Sciences (SPSS) software for windows, version 21 (SPSS Inc., Chicago, Illinois, U.S.A.).

Results

Characterization of MSCs

Cultured BM-MSCs appeared as elongated spindle-like shapes and reached confluency (80–85%) then (95–98%) after around 20 and 28 days of culture, respectively. Importantly, the immunophenotype of these cells were monitored by flow cytometry and revealed that BM-MSCs were positive for adhesion marker (CD44) and thymus cell antigen 1 (thy-1) (CD90), and negative for endothelial cell marker (CD31) and Leukocyte common antigen (CD45) which indicated that BM-MSCs were efficiently generated (Figure 2).

Characterization of MSCs-derived exosomes

The mean value of protein concentration in samples was 18.2 µg/ml. SDS-PAGE showed the presence of multiple protein bands with molecular weights 52 kDa, 65 kDa, 115 kDa and 175 kDa (Figure 3a). Scanning electron microscopy of isolated exosomes revealed spherical-shaped vesicles. The size of these exosomes was within the range of 40–80 nm in diameter (Figure 3b). The size of the exosomes and the size distribution were also recorded using dynamic light scattering. The size distribution is graphically illustrated in Figure 3c. The range of size correlates with that recorded from SEM. In addition, beads-based flow cytometry demonstrated that isolated exosomes expressed tetraspanin (CD63) (98.44%), GPI-anchored 5'nucleotidase (CD73) (98.9%) and thymus cell antigen 1 (CD90) (97.21%) (Figure 3d).

Histopathological findings

In non-infected control group, liver section showed normal hepatic architecture, polygonal hepatocytes with small rounded nuclei arranged in plates with sinusoids in-between arranged around central vein.

Early treatment with exosomes

In *S. mansoni* infected non-treated mice (GI) sacrificed 8 weeks P.I., liver sections showed multiple portal and parenchymal granulomas around *Schistosoma* ova. The

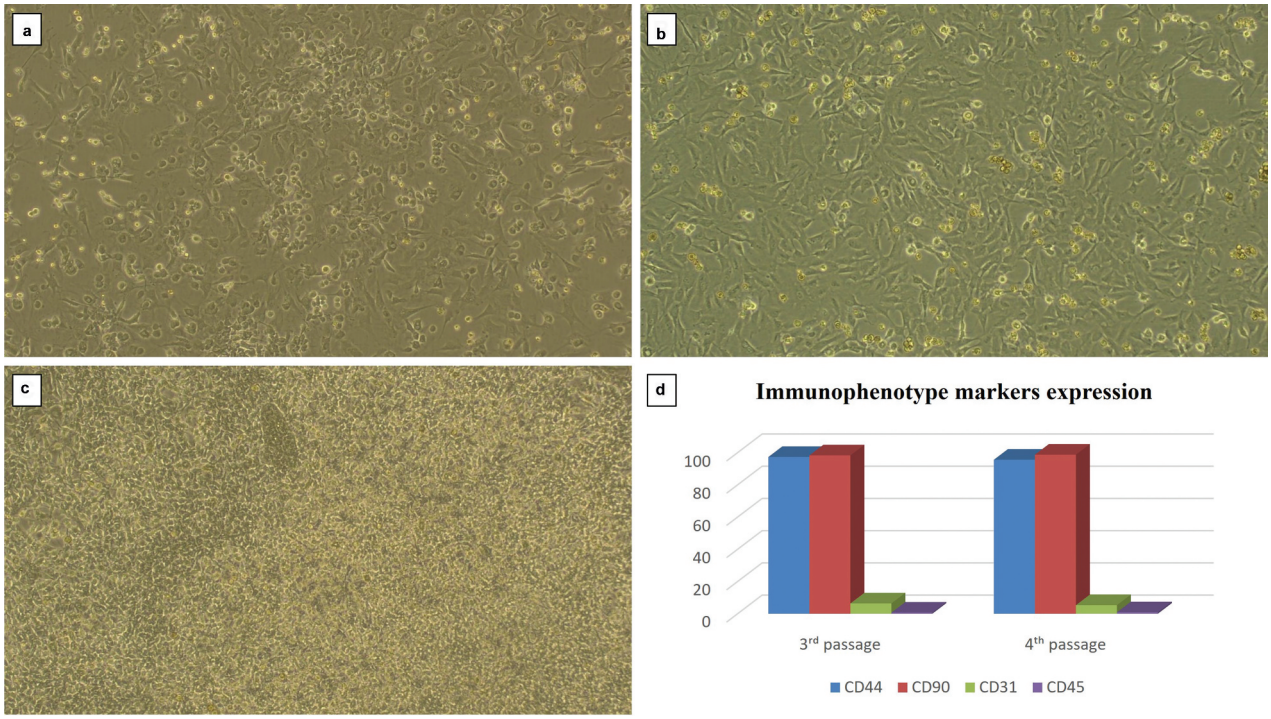

Figure 2. Isolated MSCs from murine bone marrow (a-c) (×40): (a) spindle shaped MSCs appeared after around 14 days of bone marrow culture, (b) passage 0 (initiation passage) of BM-MSCs with confluence (80–85%) reached after around 20 days of culture, (c) BM-MSCs with confluence (95–98%) reached after around 28 days of culture and (d) percentages of immunophenotype markers expression in BM-MSCs.

granulomas were of cellular and fibrocellular types with predominant inflammatory infiltrate (Figures 4a and 5a). In the PZQ-treated group (GII), multiple cellular and fibrocellular schistosomal granulomas with mild decrease in inflammatory infiltrate were observed (Figures 4b and 5b) with reduction in number (35.86%) and diameter (15.26%) of granulomas as compared to infected non-treated mice. As regards the effect of exosomes given 6 weeks P.I. on schistosomal hepatic pathology (EXO group) (GIIIa), there was a marked reduction in the number (60%) and diameter (57.12%) of granulomas in comparison to the infected control group. The majority of granulomas were of cellular types (Figures 4c and 5c). In PZQ+EXO group (GIVa), liver sections showed scanty small hepatic granulomas with marked decrease in inflammatory infiltrate. It showed the highest percentages of reduction in number (86.89%) and diameter (61.83%) of granulomas. Moreover, there was a marked improvement in hepatic pathology (Figures 4d and 5d).

The liver section of *S. mansoni* infected non-treated mice (GI) sacrificed 10 weeks P.I. showed multiple large fibrous granulomas with the cellular elements markedly decreased and replaced by concentric layers of fibrous tissue (Figures 4e and 5e). In the PZQ group (GII), liver sections showed granulomas which were fibrocellular type composed mainly of inflammatory cellular infiltrate with moderate fibrosis as compared to the infected control group (Figures 4f and 5f) with reduction in number (36.76%) and diameter (12.63%) of granulomas as compared to the infected non-treated mice. As regards exosomes-treated mice (EXO group) (GIIIa), there was a significant reduction in the number (61.76%) and the diameter (58.67%) of granuloma as compared to the infected control group. Liver sections showed cellular and fibrocellular granulomas (Figures 4g and 5g). Concerning PZQ+EXO group (GIVa), liver sections showed very scarce cellular granulomas with the highest percentages of reduction in number (87.5%) and diameter (64.8%) of granulomas. Moreover, restoration of normal liver architecture and some resolving granulomas were observed (Figures 4h and 5h).

By using image analysis of Masson's trichrome stained liver sections, there was a statistically significant difference in the percentage of liver fibrosis among all studied groups ($P < 0.001$). The reduction in the percentage of fibrosis was the highest in PZQ +EXO group (GIVa) in comparison to other groups with percentage of reduction 60.27% at 8 weeks P.I. and 73.74% at 10 weeks P.I. followed by EXO group (GIIIa) 44.67% at 8 weeks P.I. and 53.46% at 10 weeks P.I. then PZQ group (GII) (23.38% at 8 weeks P.I. and 36.1% at 10 weeks P.I.) (Table 3).

Late treatment with exosomes

Histopathological examination of hematoxylin and eosin-stained liver sections from *S. mansoni* infected non-treated mice sacrificed 12 weeks P.I. showed multiple granulomas, most of them were of fibrotic type

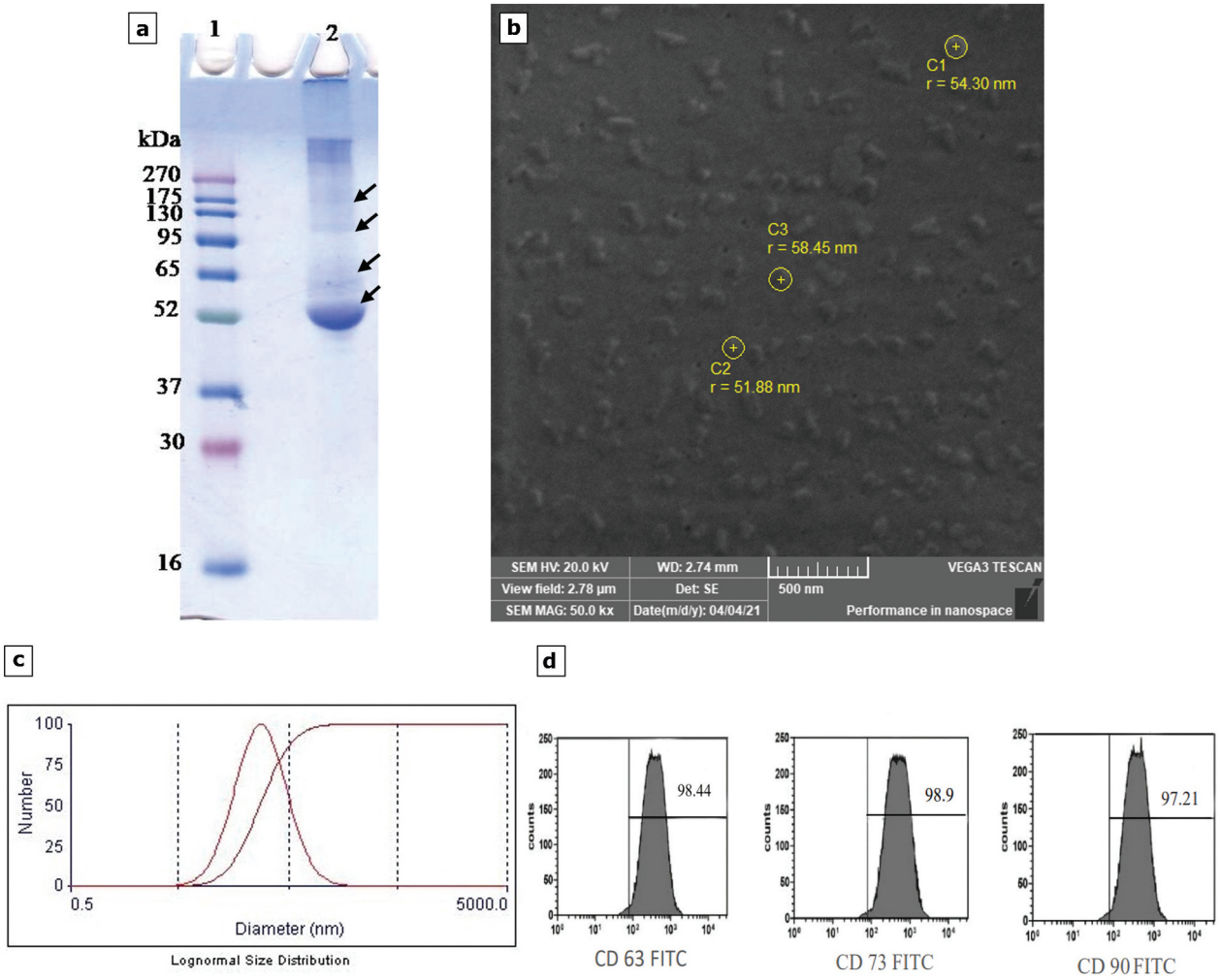

Figure 3. (a) SDS-PAGE of MSCs-derived exosomes sample (1) Molecular weight marker proteins and (2) MSCs- derived exosomes sample showed prominent protein bands with molecular weights 52 kDa, 65 kDa, 115 kDa and 175 kDa (arrows), (b) SEM of BM-MSCs-derived exosomes, radius (r), (c) vesicle size distribution chart recorded using zetasizer and (d) beads-based flow cytometry analysis of exosomes showed the presence of tetraspanin (CD63), (GPI)-anchored 5'nucleotidase (CD73) and thymus cell antigen 1 (CD90).

with centrally located concentric fibrous tissue (Figures 6a and 7a). Administration of PZQ resulted in decrease in the number of granulomas which were mainly fibrocellular type (Figures 6b and 7b) with reduction in number (30.89%) and diameter (10.44%) of granulomas as compared to infected non-treated mice. In groups treated 12 weeks P.I. either with exosomes alone (EXO group) (GIIIb) (Figures 6c and 7c) or combined with PZQ (PZQ+EXO group) (GIVb) (Figures 6d and 7d), liver sections showed improvement of the histopathological features as shown by decreased cellularity and fibrosis within the granulomas. Higher significant percentages of reduction in number and diameter were reported in PZQ+EXO group (GIVb) (88.62% and 51.77%, respectively) than in EXO group (GIIIb) (62.6% and 44.27%, respectively) as compared to infected control group.

Histopathological features of liver sections of *S. mansoni* infected non-treated mice sacrificed 14 weeks P.I. showed multiple granulomas scattered all over the liver tissue, most of them were of fibrotic type (Figures 6e and 7e). When PZQ was given, a reduction in the number (30.7%) and diameter (15.22%) of granulomas was detected as compared to the infected control group. The majority of granulomas were of fibrocellular types (Figures 6f and 7f). Regarding exosomes-treated mice (EXO group) (GIIIb), the number (64.04%) and the diameter (48.27%) of granulomas detected in liver sections were significantly reduced as compared to the infected control group. The granulomas were of fibrocellular types (Figures 6g and 7g). Liver sections of PZQ+EXO-treated group (GIVb) showed marked decrease in the number (88.59%) and diameter (59.24%) of schistosomal granulomas as compared to the other groups with the majority of them were of cellular types. As well, some resolving granulomas were detected in liver section (Figures 6h and 7h). The number and diameter of hepatic granulomas in different durations P.I. are presented in Tables 1 and 2.

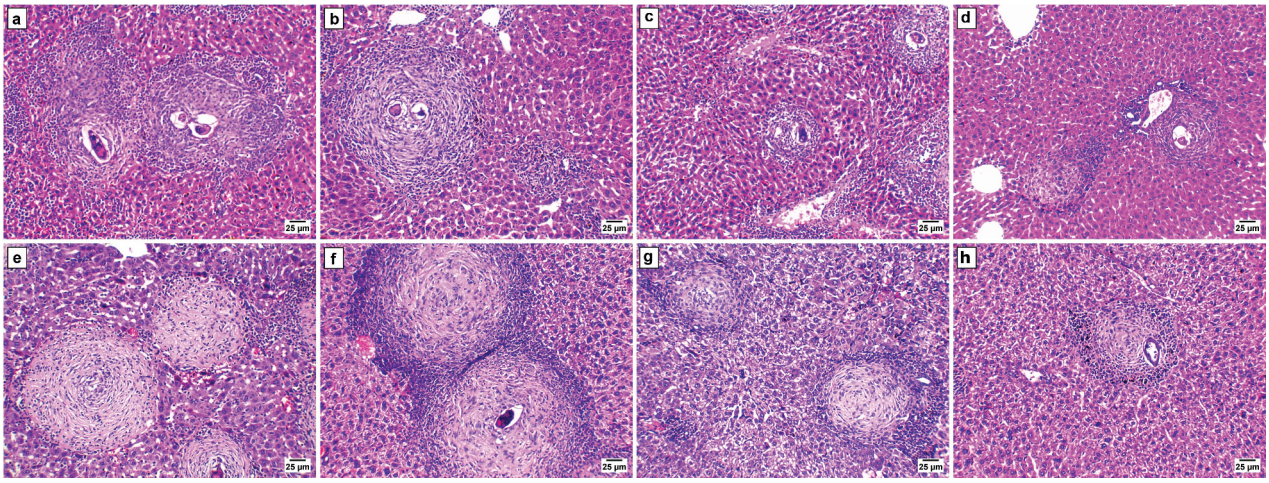

Figure 4. A photomicrograph of liver sections of *S. mansoni* infected mice 8 (a-d) and 10 (e-h) weeks P.I. (H&E × 200): (a) infected control group showing many granulomas around the ova with marked inflammatory infiltrate in the liver tissue, (b) PZQ group showing multiple schistosomal granulomas with mild decrease in inflammatory infiltrate, (c) EXO group showing noticeable decrease in the size of granulomas and moderate decrease in inflammatory infiltrate, (d) PZQ+EXO group showing few and small sized granulomas scattered among the liver tissue with marked decrease in inflammatory infiltrate, (e) infected control group showing multiple large fibrous granulomas coalescent with each other, (f) PZQ group showing granulomas coalescent with each other mainly fibrocellular, (g) EXO group showing fibrocellular granulomas and (h) PZQ+EXO group showing a single small granuloma with restoration of liver architecture.

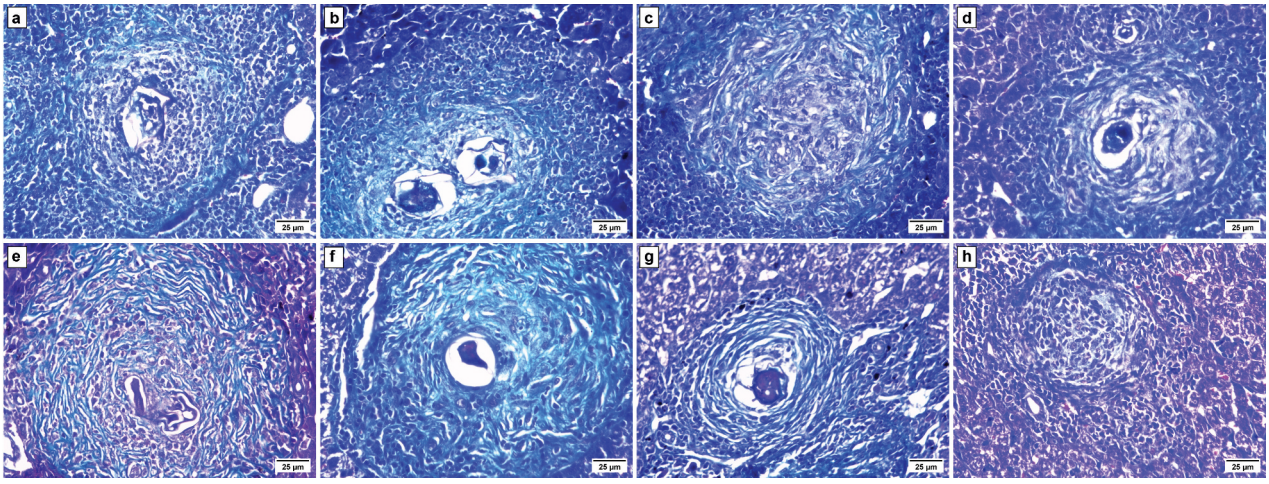

Figure 5. A Photomicrograph of Masson's trichrome stained liver sections of *S. mansoni* infected mice 8 (a-d) and 10 (e-h) weeks P. I. (MT × 400): (a) infected control group showing moderate fibrosis, (b) PZQ group showing moderate fibrosis, (c) EXO group showing mild fibrosis, (d) PZQ+EXO group showing mild fibrous tissues, (e) infected control group showing severe fibrosis, (f) PZQ group showing condensed fibrous tissues, (g) EXO group showing mild fibrosis and (h) PZQ+EXO group showing less fibrous tissues.

Morphometric analysis of Masson's trichrome stained liver sections revealed a statistically significant reduction in the percentage of fibrotic areas in all treated groups when compared to *S. mansoni* infected control groups ($P < 0.001$). The highest percentage of reduction was in PZQ+EXO group (GIVb) (62.09% at 12 weeks P.I. and 74.65% at 14 weeks P.I.) followed by EXO group (GIIIb) (47.68% at 12 weeks P.I. and 56.94% at 14 weeks P.I.) then PZQ group (GII) (28.36% at 12 weeks P. I. and 42.04% at 14 weeks P.I.) (Table 3).

Moreover, late treatment with exosomes alone (EXO group; GIIIb) or combined with PZQ (PZQ+EXO group; GIVb) exhibited comparable percentages of reduction in number of granulomas/liver section to those treated early with statistically insignificant differences at 2 and 4 weeks post treatment ($P > 0.05$). Whereas early treatment with exosomes (EXO; GIIIa and PZQ+EXO; GIVa groups) showed higher percentages of reduction in diameters of granulomas than those treated late with statistically significant differences at 2 and 4 weeks post treatment ($P < 0.001$). Interestingly, late treatment with exosomes alone (EXO group; GIIIb) and combined with PZQ (PZQ+EXO group; GIVb) achieved higher percentages of reduction in fibrosis than early treatment with exosomes (EXO; GIIIa and PZQ+EXO; GIVa groups) at 2 and 4 weeks post treatment as compared to their corresponding infected control groups (Table 4).

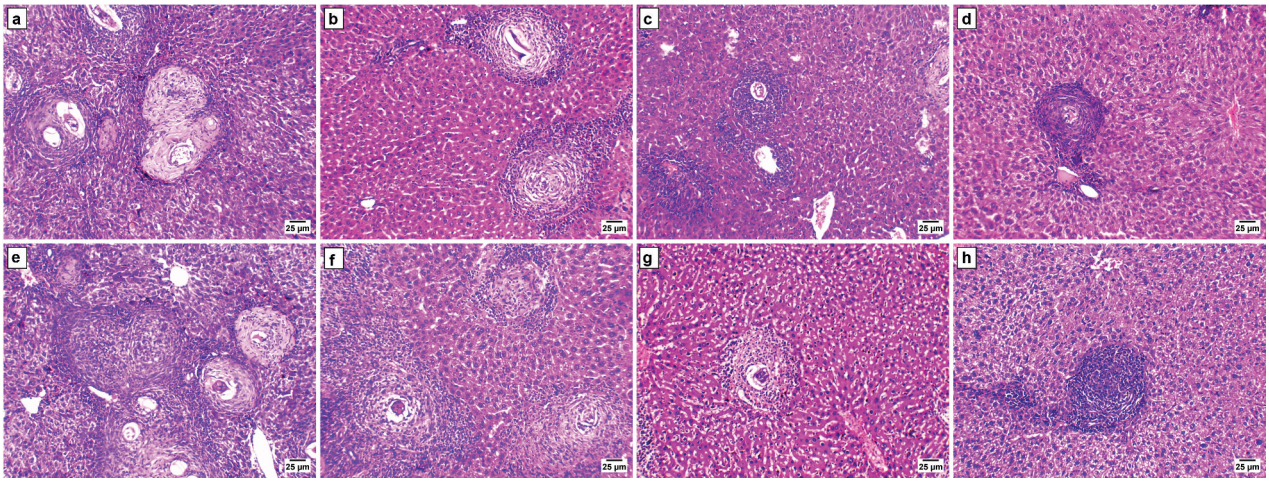

Figure 6. A photomicrograph of liver sections of *S. mansoni* infected mice 12 (a-d) and 14 (e-h) weeks P.I. (H&E × 200): (a) infected control group showing numerous granulomas mostly fibrous, (b) PZQ group showing granulomas mainly fibrocellular, (c) EXO group showing small fibrocellular granulomas and (d) PZQ+EXO group showing a single fibrocellular granuloma, (e) infected control group showing numerous fibrous granulomas scattered all over the liver tissue, (f) PZQ group showing fewer granulomas mainly fibrocellular, (g) EXO group showing a single small fibrocellular granuloma and (h) PZQ+EXO group showing a small resolving granuloma with restoration of liver architecture.

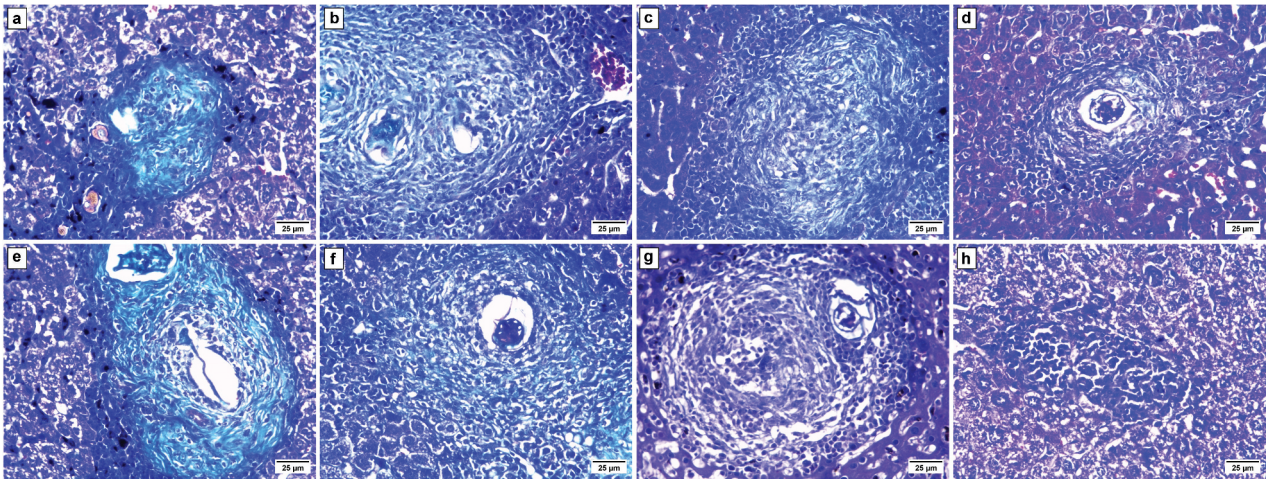

Figure 7. A Photomicrograph of Masson's trichrome stained liver sections of *S. mansoni* infected mice 12 (a-d) and 14 (e-h) weeks P.I. (MT × 400): (a) infected control group showing severe fibrosis, (b) PZQ group showing moderate fibrosis, (c) EXO group showing moderate fibrosis, (d) PZQ+EXO group showing mild fibrous tissues, (e) infected control group showing severe fibrosis, (f) PZQ group showing moderate fibrosis, (g) EXO group showing mild fibrous tissue and (h) PZQ+EXO group showing minute bands of fibrous tissue with lack of significant fibrosis.

Immunohistochemical examination of the liver

Proliferating cell nuclear antigen (PCNA)

Early treatment with exosomes. In *S. mansoni* infected control group (GI), either at 8 weeks P.I. or 10 weeks P.I., there were statistically insignificant differences in the number of positive cells of PCNA in hepatocytes in comparison to the non-infected control group ($P > 0.05$) with low expression of PCNA in hepatocytes (Figures 8a,e). In PZQ group (GII), the number of positive hepatocytes of PCNA was increased than that in the infected control group with moderate expression and showed a statistically significant difference at 10 weeks P.I. ($P < 0.05$) (Figures 8b,f). The number of PCNA positive cells in EXO (GIIIa) and PZQ +EXO (GIVa) groups of both durations P.I. was higher than infected control and PZQ groups with a statistically significant difference ($P < 0.001$), indicating an evident regeneration after exosomes treatment. PCNA showed high expression in hepatocytes in EXO (Figures 8c,g) and PZQ+EXO groups

Table 1. The number of hepatic granulomas/liver section of *S. mansoni*-infected mice in the different studied groups at different durations P.I.

	Early treatment with exosomes								Late treatment with exosomes							
	8 weeks P.I.				10 weeks P.I.				12 weeks P.I.				14 weeks P.I.			
Groups	Mean ± SD	Reduction%	F	*P*	Mean ± SD	Reduction%	F	*P*	Mean ± SD	Reduction%	F	*P*	Mean ± SD	Reduction%	F	*P*
Infected control	29.0 ± 6.6	-	74.129	0.001*	27.2 ± 6.6	-	13.778	0.001*	24.6 ± 5.3	-	94.286	0.001*	22.8 ± 5.4	-	75.449	0.001*
PZQ	18.6 ± 3.4	35.86%			17.2 ± 3.2	36.76%			17.0 ± 2.6	30.89%			15.8 ± 3.0	30.7%		
EXO	11.6 ± 2.0	60%			10.4 ± 1.6	61.76%			9.2 ± 1.2	62.6%			8.2 ± 1.2	64.04%		
PZQ+EXO	3.8 ± 1.8	86.89%			3.4 ± 1.1	87.5%			2.8 ± 1.4	88.62%			2.6 ± 1.1	88.59%		
Post Hoc Tukey	PZQ	EXO	PZQ+EXO		PZQ	EXO	PZQ+EXO		PZQ	EXO	PZQ+EXO		PZQ	EXO	PZQ+EXO	
Infected control	**0.001***	**0.001***	**0.001***		**0.001***	**0.001***	**0.001***		**0.001***	**0.001***	**0.001***		**0.001***	**0.001***	**0.001***	
PZQ	-	**0.001***	**0.001***		-	**0.001***	**0.001***		-	**0.001***	**0.001***		-	**0.001***	**0.001***	
EXO	-	-	**0.001***		-	-	**0.001***		-	-	**0.001***		-	-	**0.001***	

*statistically significant ($P < 0.05$).

Table 2. The diameter (µm) of hepatic granulomas of *S. mansoni*-infected mice in the different studied groups at different durations P.I.

	Early treatment with exosomes								Late treatment with exosomes							
	8 weeks P.I.				10 weeks P.I.				12 weeks P.I.				14 weeks P.I.			
Groups	Mean ± SD	Reduction%	F	*P*	Mean ± SD	Reduction%	F	*P*	Mean ± SD	Reduction%	F	*P*	Mean ± SD	Reduction%	F	*P*
Infected control	224.8 ± 1.56	-	15914.4	0.001*	208.3 ± 1.35	-	40376.6	0.001*	146.6 ± 2.33	-	7855.3	0.001*	138.6 ± 1.2	-	3717.2	0.001*
PZQ	190.5 ± 2.37	15.26%			182.0 ± 0.99	12.63%			131.3 ± 0.94	10.44%			117.5 ± 3.1	15.22%		
EXO	96.4 ± 1.74	57.12%			86.1 ± 0.71	58.67%			81.7 ± 0.73	44.27%			71.7 ± 1.1	48.27%		
PZQ+EXO	85.8 ± 0.93	61.83%			73.3 ± 1.11	64.81%			70.7 ± 0.40	51.77%			56.5 ± 2.1	59.24%		
Post Hoc Tukey	PZQ	EXO	PZQ+EXO		PZQ	EXO	PZQ+EXO		PZQ	EXO	PZQ+EXO		PZQ	EXO	PZQ+EXO	
Infected control	**0.001***	**0.001***	**0.001***		**0.001***	**0.001***	**0.001***		**0.001***	**0.001***	**0.001***		**0.001***	**0.001***	**0.001***	
PZQ	-	**0.001***	**0.001***		-	**0.001***	**0.001***		-	**0.001***	**0.001***		-	**0.001***	**0.001***	
EXO	-	-	**0.001***		-	-	**0.001***		-	-	**0.001***		-	-	**0.001***	

*statistically significant ($P < 0.05$).

Table 3. The percentage of liver fibrosis by Masson's trichrome stain in the different studied groups at different durations P.I.

	Early treatment with exosomes								Late treatment with exosomes							
	8 weeks P.I.				10 weeks P.I.				12 weeks P.I.				14 weeks P.I.			
Groups	Mean ± SD	Reduction%	F	*P*	Mean ± SD	Reduction%	F	*P*	Mean ± SD	Reduction%	F	*P*	Mean ± SD	Reduction%	F	*P*
Infected control	51.20 ± 0.90	-	907.318	0.001*	56.06 ± 0.67	-	2301.49	0.001*	61.28 ± 0.86	-	2085.877	0.001*	67.26 ± 0.75	-	2910.486	0.001*
PZQ	39.23 ± 1.34	23.38%			35.82 ± 1.00	36.1%			43.90 ± 0.93	28.36%			38.98 ± 1.29	42.04%		
EXO	28.33 ± 0.80	44.67%			26.09 ± 1.00	53.46%			32.06 ± 0.62	47.68%			28.96 ± 0.51	56.94%		
PZQ+EXO	20.34 ± 0.84	60.27%			14.72 ± 0.46	73.74%			23.23 ± 0.78	62.09%			17.05 ± 0.81	74.65%		
Post Hoc Tukey	PZQ	EXO	PZQ+EXO		PZQ	EXO	PZQ+EXO		PZQ	EXO	PZQ+EXO		PZQ	EXO	PZQ+EXO	
Infected control	**0.001***	**0.001***	**0.001***		**0.001***	**0.001***	**0.001***		**0.001***	**0.001***	**0.001***		**0.001***	**0.001***	**0.001***	
PZQ	-	**0.001***	**0.001***		-	**0.001***	**0.001***		-	**0.001***	**0.001***		-	**0.001***	**0.001***	
EXO	-	-	**0.001***		-	-	**0.001***		-	-	**0.001***		-	-	**0.001***	

*statistically significant ($P < 0.05$).

Table 4. Comparison of percentages of reduction in number, diameter of granulomas/liver section and fibrosis reduction in early and late treatment with exosomes, 2 and 4 weeks post treatment.

Groups		Duration P. I. in weeks	Number of granulomas			Diameter of granulomas			Fibrosis reduction		
			Mean ± SD	t	*P*	Mean ± SD	t	*P*	Mean ± SD	t	*P*
2 weeks post treatment with exosomes	**EXO**	**8 (GIIIa)**	56.65 ± 17.73	**−0.869**	**0.408**^{ns}	57.12 ± 0.72	**34.100**	**0.001***	44.64 ± 2.45	**−3.864**	**0.018***
		12 (GIIIb)	61.39 ± 7.68			44.30 ± 1.25			47.67 ± 1.28		
	PZQ +EXO	**8 (GIVa)**	85.78 ± 8.57	**−0.968**	**0.358**^{ns}	61.81 ± 0.38	**36.549**	**0.001***	60.27 ± 1.75	**−2.859**	**0.046***
		12 (GIVb)	89.00 ± 4.18			51.82 ± 0.66			62.07 ± 1.75		
4 weeks post treatment with exosomes	**EXO**	**10 (GIIIa)**	60.05 ± 8.87	**−0.156**	**0.880**^{ns}	58.65 ± 0.44	**25.004**	**0.001***	53.47 ± 1.27	**−4.449**	**0.011***
		14 (GIIIb)	61.04 ± 15.50			48.30 ± 0.93			56.94 ± 0.95		
	PZQ +EXO	**10 (GIVa)**	86.91 ± 4.51	**0.008**	**0.994**^{ns}	64.83 ± 0.38	**8.900**	**0.001***	73.74 ± 0.98	**−1.245**	**0.281**^{ns}
		14 (GIVb)	86.89 ± 8.41			59.27 ± 1.67			74.66 ± 1.14		

*statistically significant ($P < 0.05$).
^{ns}non-significant ($P > 0.05$).

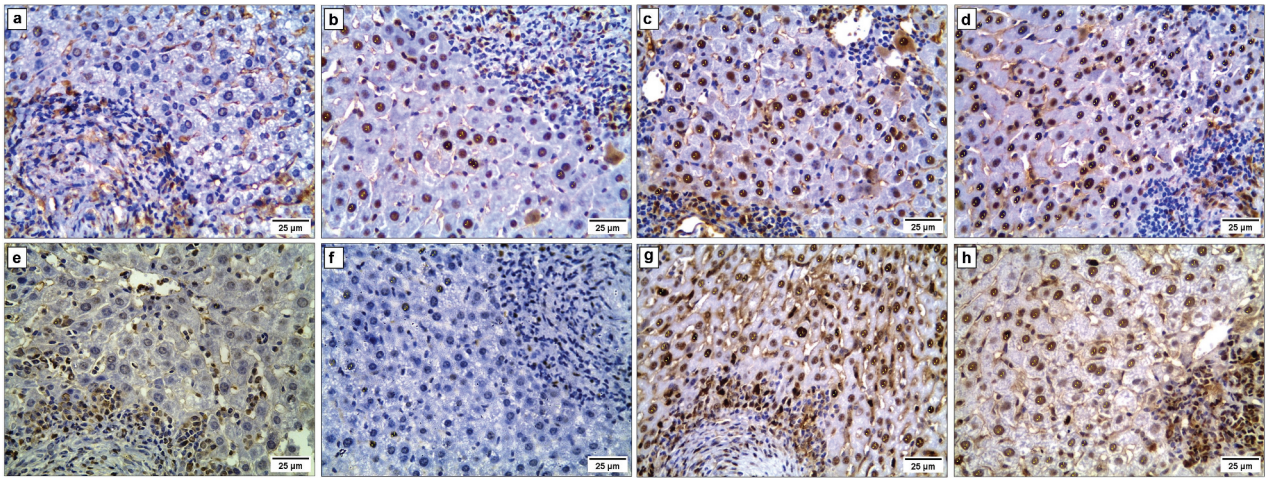

Figure 8. A photomicrograph of liver sections of *S. mansoni* infected mice 8 (a-d) and 10 (e-h) weeks P.I. for expression of PCNA in hepatocytes (positive cells are marked by yellow dots) (Immunoperoxidase × 400): (a) infected control group showing few cells with low expression of PCNA, (b) PZQ group showing moderate expression of PCNA in hepatocytes, (c) EXO group showing many positive hepatocytes with high expression of PCNA, (d) PZQ+EXO group showing many hepatocytes nuclei positive for PCNA, (e) infected control group showing low expression of PCNA in hepatocytes, (f) PZQ group showing moderate expression of PCNA in hepatocytes, (g) EXO group showing many PCNA positive hepatocytes and (h) PZQ+EXO group showing many hepatocytes with high expression of PCNA.

(Figures 8d,h). Moreover, the PZQ+EXO group of both durations P.I. showed maximal upregulation of PCNA expression in comparison to EXO group (Table 5).

Late treatment with exosomes

At 12 weeks P.I. and 14 weeks P.I., there were statistically insignificant differences in PCNA positive cells in non-infected control as compared to infected non-treated control groups ($P > 0.05$) with low expression of PCNA in hepatocytes (Figures 9a,e). In PZQ group (GII) at 12 weeks P.I., there was a statistically significant increase in PCNA expression with moderate expression as compared to infected control group ($P < 0.001$) (Figures 9b,f). The activation of hepatocytes proliferation was demonstrated in the EXO (GIIIb) and PZQ +EXO (GIVb) groups by the higher number of PCNA stained cells as compared with the other groups ($P < 0.001$). Also, there was high expression of PCNA in hepatocytes (Figures 9c,d,g,h) (Table 5).

Nuclear factor-kappa B (NF-κB)

Early treatment with exosomes. In *S. mansoni* infected control group (GI), either at 8 weeks P.I. or 10 weeks P.I., there was a statistically significant increase in the mean number of NF-κB positive cells in comparison to the non-infected control group ($P < 0.001$). NF-κB expression showed a strong positive brown staining (nuclear or cytoplasmic reaction) in the *S. mansoni* infected control group (Figures 10a,e). In PZQ group (GII) at both durations P.I., the number of NF-κB positive cells was less than that in the infected control groups of each duration P.I. with moderate staining intensity and showed a statistically significant difference ($P < 0.001$) (Figures 10b,f).

As regards EXO (GIIIa) and PZQ+EXO (GIVa) groups, there was a statistically significant decrease in the number of NF-κB positive cells as compared to infected control and PZQ groups ($P < 0.001$) with weak nuclear or cytoplasmic staining intensity at both 8 and 10 weeks P.I. (Figures 10c,g). The maximal reduction of NF-κB positive cells was observed in PZQ+EXO group

Table 5. The mean number of PCNA positive cells in the liver of mice in the different studied groups at different durations P.I.

	Early treatment with exosomes								Late treatment with exosomes							
	8 weeks P.I.				10 weeks P.I.				12 weeks P.I.				14 weeks P.I.			
Groups	Mean ± SD		F	*P*	Mean ± SD		F	*P*	Mean ± SD		F	*P*	Mean ± SD		F	*P*
Non-infected control	7 ± 1		167.57	0.001*	7 ± 1		197.73	0.001*	7 ± 1		559.26	0.001*	7 ± 1		120.182	0.001*
Infected control	2 ± 1				2 ± 2				2 ± 1				2 ± 1			
PZQ	13 ± 3				14 ± 4				14 ± 2				16 ± 3			
EXO	54 ± 5				57 ± 5				61 ± 4				70 ± 16			
PZQ+EXO	74 ± 11				77 ± 10				74 ± 5				83 ± 7			
Post Hoc Tukey	Infected control	PZQ	EXO	PZQ +EXO	Infected control	PZQ	EXO	PZQ+EXO	Infected control	PZQ	EXO	PZQ+EXO	Infected control	PZQ	EXO	PZQ+EXO
Non-infected control	**0.656**^{ns}	**0.631**^{ns}	**0.001***	**0.001***	**0.693**^{ns}	**0.246**^{ns}	**0.001***	**0.001***	**0.221**^{ns}	**0.009***	**0.001***	**0.001***	**0.843**^{ns}	**0.341**^{ns}	**0.001***	**0.001***
Infected control	-	**0.30**^{ns}	**0.001***	**0.001***	-	**0.02***	**0.001***	**0.001***	-	**0.001***	**0.001***	**0.001***	-	**0.056**^{ns}	**0.001***	**0.001***
PZQ	-	-	**0.001***	**0.001***	-	-	**0.001***	**0.001***	-	-	**0.001***	**0.001***	-	-	**0.001***	**0.001***
EXO	-	-	-	**0.001***	-	-	-	**0.001***	-	-	-	**0.001***	-	-	-	**0.098**^{ns}

*statistically significant ($P < 0.05$).
^{ns}non-significant ($P > 0.05$).

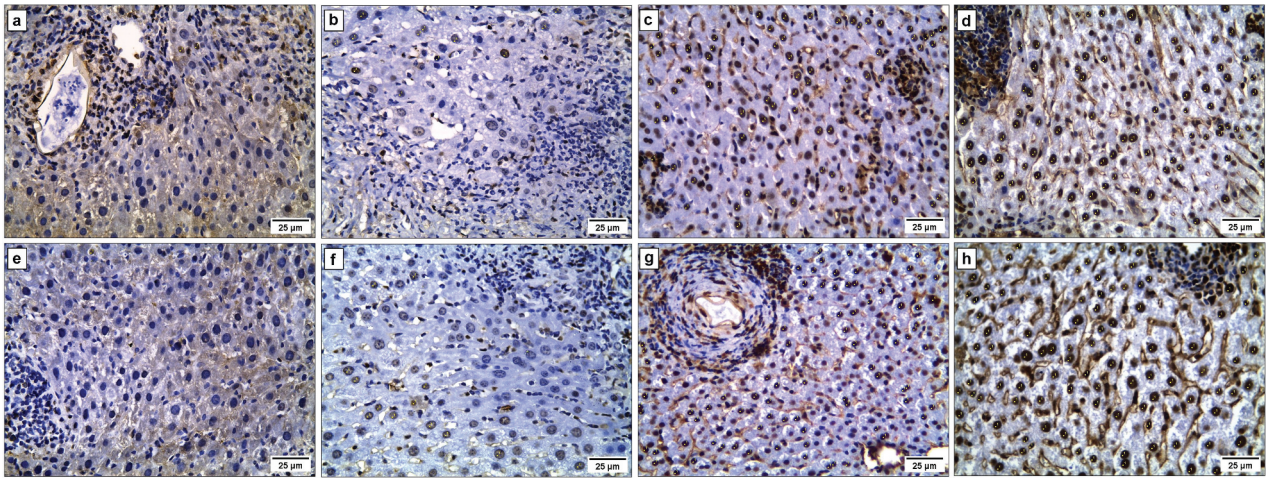

Figure 9. A Photomicrograph of liver sections of *S. mansoni* infected mice 12 (a-d) and 14 (e-h) weeks P.I. for expression of PCNA in hepatocytes (positive cells are marked by yellow dots) (Immunoperoxidase × 400): (a) infected control group showing few cells with low expression of PCNA, (b) PZQ group showing moderate expression of PCNA in hepatocytes, (c) EXO group showing many cells with high expression of PCNA, (d) PZQ+EXO group showing many hepatocytes nuclei positive for PCNA, (e) infected control group showing few cells with low expression of PCNA, (f) PZQ group showing moderate expression of PCNA in hepatocytes, (g) EXO group showing many PCNA positive hepatocytes and (h) PZQ+EXO group showing many hepatocytes nuclei positive for PCNA.

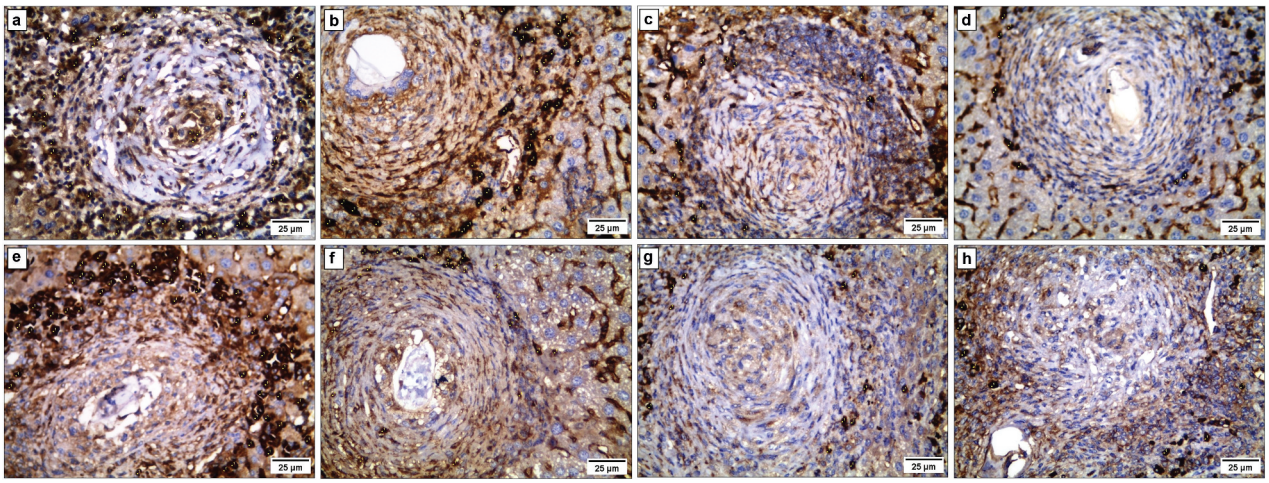

Figure 10. A Photomicrograph of liver sections of *S. mansoni* infected mice 8 (a-d) and 10 (e-h) weeks P.I. for expression of NF-κB (positive cells are marked by yellow dots) (Immunoperoxidase × 400): (a) infected control group showing strong positive immunoreaction for NF-κB, (b) PZQ group showing moderate staining intensity, (c) EXO group showing weak staining intensity, (d) PZQ+EXO group showing very weak NF-κB immunostaining, (e) infected control group showing strong positive immunoreaction for NF-κB, (f) PZQ group showing moderate staining intensity, (g) EXO group showing weak staining intensity and (H) PZQ +EXO group showing very weak NF-κB immunostaining.

at 10 weeks P.I. with a statistically insignificant difference compared to the non-infected control group ($P > 0.05$) (Figures 10d,h) (Table 6).

Late treatment with exosomes

At 12 weeks P.I. or 14 weeks P.I., the mean number of NF-κB positive cells were significantly upregulated with strong staining intensity in *S. mansoni* infected control groups compared to the non-infected control groups (Figures 11a,e). Concerning PZQ group (GII) at both durations P.I., there was a statistically significant reduction in the number of NF-κB positive cells with moderate staining intensity as compared to other groups ($P < 0.001$) (Figures 11b,f).

Treatment with exosomes (EXO; GIIIb and PZQ+EXO; GIVb groups) significantly reduced the number of NF-κB positive cells with statistically significant differences as compared to other groups at 12 and 14 weeks P.I. ($P < 0.05$) with weak nuclear or cytoplasmic staining intensity (Figures 11c,g). More reduction in the number and staining intensity of NF-κB positive cells was observed in PZQ+EXO group at 14 weeks P.I. with a statistically insignificant difference compared to the non-infected control group ($P > 0.05$) (Figures 11d,h) (Table 6).

Table 6. The mean number of NF-κB positive cells in the liver of mice in the different studied groups at different durations P.I.

	Early treatment with exosomes								Late treatment with exosomes							
	8 weeks P.I.				10 weeks P.I.				12 weeks P.I.				14 weeks P.I.			
Groups	Mean ± SD		F	*P*	Mean ± SD		F	*P*	Mean ± SD		F	*P*	Mean ± SD		F	*P*
Non-infected control	4 ± 2		581.25	0.001*	4 ± 2		293.59	0.001*	4 ± 2		620.824	0.001*	4 ± 2		346.086	0.001*
Infected control	63 ± 2				52 ± 4				55 ± 2				51 ± 4			
PZQ	38 ± 3				31 ± 2				36 ± 2				34 ± 2			
EXO	15 ± 1				14 ± 1				16 ± 2				11 ± 2			
PZQ+EXO	10 ± 3				8 ± 3				9 ± 2				7 ± 2			
Post Hoc Tukey	Infected control	PZQ	EXO	PZQ+EXO	Infected control	PZQ	EXO	PZQ+EXO	Infected control	PZQ	EXO	PZQ+EXO	Infected control	PZQ	EXO	PZQ+EXO
Non-infected control	**0.001***	**0.001***	**0.001***	**0.003***	**0.001***	**0.001***	**0.001***	**0.107**^{ns}	**0.001***	**0.001***	**0.001***	**0.009***	**0.001***	**0.001***	**0.003***	**0.333**^{ns}
Infected control	-	**0.001***	**0.001***	**0.001***	-	**0.001***	**0.001***	**0.001***	-	**0.001***	**0.001***	**0.001***	-	**0.001***	**0.001***	**0.001***
PZQ	-	-	**0.001***	**0.001***	-	-	**0.001***	**0.001***	-	-	**0.001***	**0.001***	-	-	**0.001***	**0.001***
EXO	-	-	-	**0.03***	-	-	-	**0.03***	-	-	-	**0.001***	-	-	-	**0.180**^{ns}

*statistically significant ($P < 0.05$).
^{ns}non-significant ($P > 0.05$).

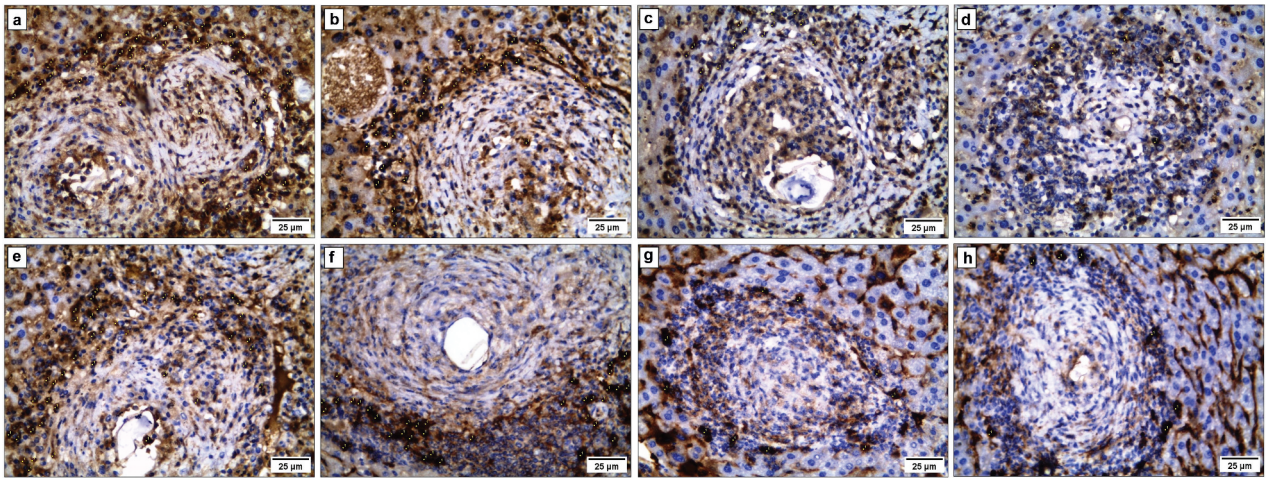

Figure 11. A Photomicrograph of liver sections of *S. mansoni* infected mice 12 (a-d) and 14 (e-h) weeks P.I. for expression of NF-κB (positive cells are marked by yellow dots) (Immunoperoxidase × 400): (a) infected control group showing strong expression of NF-κB immunostaining, (b) PZQ group showing moderate expression of NF-κB immunostaining, (c) EXO group showing weak staining intensity, (d) PZQ+EXO group showing very weak NF-κB immunostaining, (e) infected control group showing strong expression of NF-κB immunostaining, (f) PZQ group showing moderate expression of NF-κB immunostaining, (g) EXO group showing weak staining intensity and (h) PZQ+EXO group showing very weak NF-κB immunostaining.

Discussion

Schistosomiasis is considered the world's second most important parasitic disease after malaria regarding public health and socio-economic effects [38]. Currently, there are still no efficacious therapeutic options for schistosomiasis-induced liver fibrosis [7]. Consequently, developing strategies is crucial for preventing or treating liver fibrosis.

In this study, MSCs were successfully isolated from bone marrow as confirmed by their appearance as adherent long spindle-like cells. According to the guiding principles of the International Society of Cell Therapy, BM-MSCs express surface markers including CD90, CD105, CD44 and CD73, but do not express CD45, CD31, CD34, CD19 and CD14 [39,40]. By flow cytometry, the isolated MSCs of the current work positively expressed CD44 and CD90, whereas they were negative for CD31 and CD45 expression.

Then, we successfully isolated exosomes from BM-MSCs by differential ultracentrifugation. Cultured fluid samples revealed the presence of spherical-shaped protein-containing nanovesicles with 40–80 nm in diameter confirming that these nanovesicles are exosomes. This is consistent with the range of exosomes particle sizes. Similarly, Chen et al. [23] and Lu et al. [41] stated that isolated exosomes from BM-MSCs culture supernatants showed small membrane vesicles sized from 30 to 100 nm in diameter by electron microscopy.

In the present study, SDS-PAGE showed the presence of multiple bands at 52 kDa, 65 kDa, 115 kDa and 175 kDa proteins. These findings are consistent with the results of Ko et al. [42] who reported that exosomes isolated from adipose-derived MSCs showed the presence of exosomal proteins presented mainly as 38 kDa, 60 kDa, 80 kDa, 100 kDa and 180 kDa gel bands.

In the current study, isolated exosomes were further characterized for the presence of specific exosomal surface markers. They expressed tetraspanins (CD63), glycosylphosphatidylinositol (GPI)-anchored 5'nucleotidase (CD73) and thymus cell antigen 1 (CD90). Ohno et al. [43] stated that the most common exosomal surface proteins are members of the tetraspanin family, a group of scaffold membrane proteins. CD63 is one of tetraspanins which is considered as a set of proteins packaged into exosomes during biogenesis [44]. Tetraspanins are involved in cellular interactions through binding with various proteins, such as integrins and major histocompatibility complex molecules [45]. Moreover, they are expressed on the membrane of MSCs-derived exosomes [46]. This was in line with previous studies in which western blot analysis indicated that BM-MSCs-derived exosomes were positive for CD63 [23,41,47].

Furthermore, MSCs-derived exosomes express CD73 and CD90 which are characteristic of MSCs [48]. CD73 is a cell surface glycosylphosphatidylinositol-anchored glycoprotein that plays a key role in the balance between inflammation and immune suppression [49,50]. CD90, also known as Thy-1, is an integrin ligand or receptor which regulates cell–cell and cell–extracellular matrix interactions [51]. Likewise, these findings are consistent with the results of Dong et al. [52] who found that human umbilical cord MSCs-derived extracellular vesicles expressed CD90 and CD73.

Our results showed that the number and diameter of hepatic granulomas were significantly reduced after treatment with PZQ with minimal antifibrotic effect as

compared to that of *S. mansoni* infected control group. These findings are in accordance with Abou Rayia et al. [53] and Elmalawany et al. [54] who reported that *S. mansoni* infected mice treated with PZQ showed a reduction in the number and size of the hepatic granulomas with moderate inflammatory cellular infiltrate. Similarly, Ma et al. [55] showed reduction in collagen deposition in the liver in *S. japonicum* infected mice treated with PZQ. However, Nono et al. [56] also indicated that PZQ failed to reverse established fibrosis in chronic murine schistosomiasis.

Concerning the effects on the number and diameter of hepatic granulomas in case of early treatment with exosomes, data from the present study showed that there was a statistically significant reduction in EXO group at 8 and 10 weeks P.I. in comparison with the infected control and PZQ groups. Additionally, PZQ +EXO groups significantly reduced the number of granulomas as well as granuloma diameter in the liver at both durations P.I. The percentages of reduction were significantly higher than those of EXO- and PZQ-treated groups. In the meantime, late treatment with exosomes revealed that the number and diameter of hepatic granulomas were significantly reduced in EXO and PZQ+EXO groups as compared to other groups at both durations of sacrifice with more reduction in the PZQ+EXO group.

Moreover, the EXO and PZQ+EXO-treated groups in case of early and late treatment with exosomes showed marked improvement in hepatic pathology with marked decrease in the inflammatory cells and fibrosis than infected control and PZQ-treated groups. It is noticeable that more improvement was observed when exosomes were combined with PZQ suggesting that combination could greatly increase the effect of PZQ for repairing liver fibrosis induced by *S. mansoni*.

These findings are consistent with the results of Dong et al. [52] who reported that human umbilical cord MSCs-derived extracellular vesicles injection (2×10^9) at the 4th week after *S. japonicum* infection significantly decrease the formation of hepatic granulomas at 6 or 8 weeks after infection leading to improvement of liver granuloma and significantly reduced collagen deposition and fibrosis in treated mice as compared to infected control group. Moreover, their combination with PZQ showed significant reduction in granuloma formation and the severity of liver fibrosis at 10 weeks after infection. MSCs-derived extracellular vesicles could be efficient for suppressing hepatic stellate cells activation, improving hepatic cell regeneration and reducing liver injury and fibrosis.

In the same context, umbilical cord MSCs-derived exosomes could improve liver injury [57]. They could ameliorate carbon tetrachloride (CCl4)-induced liver fibrosis by reducing the surface fibrous capsules and softening their texture, decreasing hepatic inflammation and inhibiting collagen production in the CCl4-induced fibrotic liver [58]. The same effects were reported by the administration of human BM-MSCs-derived exosomes [59]. Moreover, several other studies have investigated the antifibrotic activity of MSCs-derived extracellular vesicles in various *in vivo* models of liver fibrosis [52,60,61]. These results could be explained by the ability of MSCs-derived exosomes to attenuate macrophage infiltration and local liver damage and diminish the serum levels of inflammatory factors, thus improving liver histology and enhancing liver injury [62].

It is worth mentioning that treatment of schistosomiasis mansoni by BM-MSCs at 8 weeks P.I. either alone or combined with PZQ was in agreement with our present results. They improved the histopathological changes in the liver including diminution in the mean diameter and number of granulomas, reduction of inflammatory cellular infiltration and significant decrease in fibrous tissue in comparison to the infected group. The decrease was more obvious when used with PZQ [10,53,63].

Particular attention is paid to the antifibrotic properties of BM-MSCs, including the inhibition of collagen fiber deposition [64]. Santiago et al. [65] have reported increased levels of matrix metalloproteinase, which may directly degrade the extracellular matrix causing apoptosis of hepatic stellate cells. Indeed, exosomes orchestrate the principal mechanisms of action of MSCs after infusion. The use of MSCs-derived exosomes may provide considerable advantages over their counterpart live cells, potentially reducing undesirable side effects [15].

Hegab et al. [10] suggested that the reduction observed in the number of liver granulomas after BM-MSCs treatment in schistosomiasis, may be due to paracrine factors secreted by stem cells, affecting the parasite maturation and/or fecundity. Furthermore, Etewa et al. [66] found that MSCs affected adult worms and caused reduction in the number and size of liver granulomas. These suggested mechanisms may explain how treatment with MSCs-derived exosomes reduces the number of granulomas in our study. They could affect adult fecundity leading to decrease in the total egg burden. Yet, it needs further investigations.

Since PZQ treatment caused a high eradication percentage of *Schistosoma* adult worms and decreased egg deposition [67], the best results in the current study were obtained when MSCs-derived exosomes were given with PZQ. This could be attributed to the elimination of adult worms and reduction of eggs deposited by PZQ added to the reduction of fibrosis by MSCs-derived exosomes.

Surprisingly, late treatment with exosomes alone (EXO group) or combined with PZQ (PZQ+EXO group) in the current study achieved higher percentages of

reduction in fibrosis than in early treatment with exosomes. This better outcome is mostly due to its anti fibrotic effect. Thus, this study provided evidence that treatment with exosomes can reduce morbidity during early and late *S. mansoni* infection in mice.

In the present study, PCNA immune-staining technique was used to evaluate liver regeneration after treatment with exosomes. Evident increase of PCNA expression was observed in EXO and PZQ+EXO-treated groups in case of early and late treatment of exosomes in comparison with other groups of each duration P. I. with more increase in PZQ+EXO group. Similar results were reported by Tan et al. [68] who investigated the effect of MSCs-derived exosomes in an established CCl4-induced liver injury mouse model. The administration of MSCs-derived exosomes was found to reverse the induced liver injury in mice with active proliferation of hepatocytes in exosomes treatment group as shown by high expression of proliferation proteins (PCNA) and the anti-apoptotic gene Bcl-xL [68].

Rong et al. [59] suggested that hepatocyte regeneration was increased under the effect of exosomes via inhibition of hepatic stellate cell activation. The hepatoprotective effects of MSCs-derived exosomes relied on the suppression of caspase-3-driven apoptosis and on inhibition of caspase-1-induced pyroptosis of hepatocytes. Moreover, they may increase hepatocyte number by inducing sphingosine kinase-dependent activation of sphingosine-1-phosphate that improve hepatocyte growth, survival and proliferation [69].

This finding is consistent with the function of BM-MSCs. Yannaki et al. [70] suggested that BM-MSCs might promote self-proliferation and endogenous liver regeneration through secretion of growth factors. Besides, while investigating their effect on treatment of CCL4-induced liver fibrosis in rats, the number of PCNA positive hepatocytes was significantly higher in the BM-MSCs-treated group as compared to control group [71,72].

The current work showed marked increase in NF-κB expression in *S. mansoni* infected non-treated groups at all durations P.I. There is a lot of evidence that NF-κB activation is linked to *Schistosoma*-induced fibrosis [73]. Upon liver injury, induction of NF-κB occurs leading to production of various inflammatory factors including interleukin 6 (IL-6) and tumor necrosis factor-alpha (TNF-α). Activation of NF-κB would contribute to massive hepatocytes death, inflammation and activation of hepatic stellate cells leading to fibrosis [74]. Moreover, Gong et al. [75] suggested that reduced NF-κB activity might prevent *Schistosoma* induction of fibrosis. The present study showed evident reduction of NF-κB expression was observed in all treated groups, but it was lower in PZQ+EXO-treated groups at all durations P.I.

Similar observations were also made by Saad El-Din et al. [76] who demonstrated that NF-κB expression was reduced in *S. mansoni* infected mice treated with PZQ. Moreover, the anti-inflammatory effect of PZQ has been reported in schistosomiasis mansoni treatment by reduction of proinflammatory cytokines expression in the liver [77]. Thus, in the current work, exosomes could potentiate the anti-inflammatory effect of PZQ in PZQ+EXO group. MSCs-derived exosomes suppress the production of inflammatory phenotype in Kupffer cells and their cytokines (TNF-α, IL-1β and IL-6) in liver and decrease their cross-talk with pro-fibrotic hepatic stellate cells, which are the cells responsible for fibrosis and collagen production in the liver tissues. Moreover, they suppress the expression of pro-fibrotic genes (collagen I, vimentin, alpha-smooth muscle actin and fibronectin) in hepatic stellate cells and subsequently improve liver fibrosis [65,78]. As a result, lower NF-κB expression in the treated groups in the current study might be implicated in reduced fibrosis, reduction in the size of the granulomas and inflammation of the liver as compared to infected control group.

NF-κB is regulated by interaction with a family of regulatory proteins. The inhibitor of nuclear factor κB (IκB) proteins may be stimulated by many factors, such as TNF-α, *via* the phosphorylation and degradation of IκB [79]. MSCs-derived extracellular vesicles significantly reduced expression of inflammatory cytokines (TNF-α) in the liver tissue [60]. Similarly, MSCs-derived extracellular vesicles caused immunomodulatory effects by decreasing the gene expression of pro-inflammatory cytokines (TNF-α) in liver tissues in a thioacetamide-induced chronic liver injury rat model [80]. Subsequently, this is considered as a suggested mechanism for suppression of NF-κB by MSCs-derived exosomes.

To sum up, the present work demonstrates, for the first time, the possible ameliorative outcome of exosomes derived from BM-MSCs on schistosomiasis-induced liver fibrosis. Injection of BM-MSCs-derived exosomes into *S. mansoni*-infected mice resulted in reduction in number and diameter of granulomas, reduction in inflammation, regression of liver fibrosis and proliferation of new hepatocytes. Moreover, MSCs-derived exosomes enhanced the beneficial effects of PZQ therapy. Therefore, combining MSCs derived exosomes with PZQ greatly improved the efficacy of PZQ for repairing *S. mansoni*-induced hepatic fibrosis, suggesting that MSCs-derived exosomes can be utilized as an effective adjuvant for attenuation of liver fibrosis caused by schistosomiasis. Furthermore, we suggested a novel mechanism for MSCs-derived exosomes mediated tissue repair through their antifibrotic, anti-inflammatory and regenerative effects that hopefully become a promising alternative to MSCs for transplantation therapy.

Disclosure statement

No potential conflict of interest was reported by the author(s).

Funding

This study was not funded by any research grant.

ORCID

Asmaa R. Ellakany http://orcid.org/0000-0001-5272-8464

References

[1] Carbonell C, Rodríguez-Alonso B, López-Bernús A, et al. Clinical spectrum of schistosomiasis: an update. J Clin Med. 2021;10(23):5521. doi: 10.3390/jcm10235521

[2] Nepal P, Ojili V, Songmen S, et al. Multisystem imaging review of human schistosomiasis: characteristic imaging findings. Clin Imaging. 2019;54:163–171. doi:10.1016/j.clinimag.2019.01.011

[3] Zheng B, Zhang J, Chen H, et al. T lymphocyte-mediated liver immunopathology of schistosomiasis. Front Immunol. 2020;11:61. doi:10.3389/fimmu.2020.00061

[4] Chen Q, Zhang J, Zheng T, et al. The role of microRnas in the pathogenesis, grading and treatment of hepatic fibrosis in schistosomiasis. Parasites Vectors. 2019;12(1):611. doi:10.1186/s13071-019-3866-0

[5] Mäder P, Rennar GA, Ventura AMP, et al. Chemotherapy for fighting schistosomiasis: past, present and future. ChemMedchem. 2018;13(22):2374–2389. doi: 10.1002/cmdc.201800572

[6] El-Beshbishi SN, Saleh NE, Abd El-Mageed SA, et al. Effect of omega-3 fatty acids administered as monotherapy or combined with artemether on experimental *Schistosoma mansoni* infection. Acta Trop. 2019;194:62–68. doi:10.1016/j.actatropica.2019.02.027

[7] Fang H, Yu L, You D, et al. *In vivo* Therapeutic effects and mechanisms of hydroxyasiaticoside combined with praziquantel in the treatment of schistosomiasis induced hepatic fibrosis. Front Bioeng Biotechnol. 2021;8:613784. doi:10.3389/fbioe.2020.613784

[8] Al-Dhamin Z, Liu LD, Li DD, et al. Therapeutic efficiency of bone marrow-derived mesenchymal stem cells for liver fibrosis: A systematic review of *in vivo* studies. World J Gastroenterol. 2020;26(47):7444–7469. doi: 10.3748/wjg.v26.i47.7444

[9] Abou Rayia D, Elmarhoumy S, Ismail H, et al. The outcomes of bone marrow stromal cell therapy in schistosomal hepatic fibrosis: An experimental study. J Egypt Soc Parasitol. 2017;47(3):633–642. doi: 10.21608/jesp.2017.77722

[10] Hegab MH, Abd-Allah SH, Badawey MS, et al. Therapeutic potential effect of bone marrow-derived mesenchymal stem cells on chronic liver disease in murine schistosomiasis *mansoni*. J Parasit Dis. 2018;42(2):277–286. doi: 10.1007/s12639-018-0997-8

[11] Fennema EM, Tchang LAH, Yuan H, et al. Ectopic bone formation by aggregated mesenchymal stem cells from bone marrow and adipose tissue: A comparative study. J Tissue Eng Regen Med. 2018;12(1):e150–e158. doi: 10.1002/term.2453

[12] Regmi S, Pathak S, Kim JO, et al. Mesenchymal stem cell therapy for the treatment of inflammatory diseases: Challenges, opportunities, and future perspectives. Eur J Cell Biol. 2019;98(5–8):151041. doi: 10.1016/j.ejcb.2019.04.002

[13] Harrell CR, Fellabaum C, Jovicic N, et al. Molecular mechanisms responsible for therapeutic potential of mesenchymal stem cell-derived secretome. Cells. 2019;8(5):467. doi: 10.3390/cells8050467

[14] Janockova J, Slovinska L, Harvanova D, et al. New therapeutic approaches of mesenchymal stem cells-derived exosomes. J Biomed Sci. 2021;28(1):39. doi: 10.1186/s12929-021-00736-4

[15] Mendt M, Rezvani K, Shpall E. Mesenchymal stem cell-derived exosomes for clinical use. Bone Marrow Transplant. 2019;54(S2):789–792. doi: 10.1038/s41409-019-0616-z

[16] Zhou Y, Yamamoto Y, Xiao Z, et al. The immunomodulatory functions of mesenchymal stromal/stem cells mediated via paracrine activity. J Clin Med. 2019;8(7):1025. doi: 10.3390/jcm8071025

[17] Qiu G, Zheng G, Ge M, et al. Functional proteins of mesenchymal stem cell-derived extracellular vesicles. Stem Cell Res Ther. 2019;10(1):1–11. doi: 10.1186/s13287-019-1484-6

[18] Cheng Y, Zeng Q, Han Q, et al. Effect of pH, temperature and freezing-thawing on quantity changes and cellular uptake of exosomes. Protein Cell. 2019;10(4):295–299. doi: 10.1007/s13238-018-0529-4

[19] Filho DM, de Carvalho Ribeiro P, Oliveira LF, et al. Enhancing the therapeutic potential of mesenchymal stem cells with the CRISPR-Cas System. Stem Cell Rev And Rep. 2019;15(4):463–473. doi: 10.1007/s12015-019-09897-0

[20] Baharlooi H, Azimi M, Salehi Z, et al. Mesenchymal stem cell-derived exosomes: a promising therapeutic ace card to address autoimmune diseases. Int J Stem Cells. 2020;13(1):13–23. doi: 10.15283/ijsc19108

[21] Liu H, Liang Z, Wang F, et al. Exosomes from mesenchymal stromal cells reduce murine colonic inflammation via a macrophage-dependent mechanism. JCI Insight. 2019;4(24):e131273. doi: 10.1172/jci.insight.131273

[22] Xunian Z, Kalluri R. Biology and therapeutic potential of mesenchymal stem cell-derived exosomes. Cancer Sci. 2020;111(9):3100–3110. doi: 10.1111/cas.14563

[23] Chen L, Lu FB, Chen DZ, et al. Bmscs-derived miR-223-containing exosomes contribute to liver protection in experimental autoimmune hepatitis. Mol Immunol. 2018;93:38–46. doi:10.1016/j.molimm.2017.11.008

[24] Ahmad A, Shakoori A. Cytotoxic effect of cigarette smoke condensate on mice and rat mesenchymal stem cells and HeLa cells. Turk J Med Sci. 2012;42(1):1–5. doi: 10.3906/sag-1105-19

[25] Gang EJ, Jeong JA, Han S, et al. *In vitro* endothelial potential of human UC blood-derived mesenchymal stem cells. Cytotherapy. 2006;8(3):215–227. doi: 10.1080/14653240600735933

[26] Théry C, Amigorena S, Raposo G, et al. Isolation and characterization of exosomes from cell culture supernatants and biological fluids. Curr Protoc Cell Biol. 2006;30(1):3–22. doi: 10.1002/0471143030.cb0322s30

[27] Nowakowski AB, Wobig WJ, DH P. Native SDS-PAGE: high resolution electrophoretic separation of proteins with retention of native properties including bound metal ions. Metallomics. 2014;6(5):1068–1078. doi: 10.1039/C4MT00033A

[28] Sokolova V, Ludwig AK, Hornung S, et al. Characterisation of exosomes derived from human cells by nanoparticle tracking analysis and scanning electron microscopy. Colloids Surf B Biointerfaces. 2011;87(1):146–150. doi: 10.1016/j.colsurfb.2011.05.013

[29] Chernyshev VS, Rachamadugu R, Tseng YH, et al. Size and shape characterization of hydrated and

desiccated exosomes. Anal Bioanal Chem. 2015;407 (12):3285–3301. doi: 10.1007/s00216-015-8535-3
[30] Théry C, Witwer KW, Aikawa E, et al. Minimal information for studies of extracellular vesicles 2018 (MISEV2018): a position statement of the international society for extracellular vesicles and update of the MISEV2014 guidelines. J Extracell Vesicles. 2018;7 (1):1535750. doi: 10.1080/20013078.2018.1535750
[31] Suárez H, Gámez-Valero A, Reyes R, et al. A bead-assisted flow cytometry method for the semi-quantitative analysis of extracellular Vesicles. Sci Rep. 2017;7(1):11271. doi: 10.1038/s41598-017-11249-2
[32] Holanda JC, Pellegrino J, Gazzinelli G. Infection of mice with cercariae and schistosomula of *Schistosoma mansoni* by intravenous and subcutaneous routes. Rev Inst Med Trop. 1974;16(3):132–134.
[33] Nessim NG, Demerdash Z. Correlation between infection intensity, serum immunoglobulin profile, cellular immunity and the efficacy of treatment with praziquantel on murine schistosomiasis *mansoni*. Arzneimittelforschung. 2000;50(2):173–177. doi: 10.1055/s-0031-1300185
[34] Bancroft JD, Steven A. Histopathological stains and their diagnostic uses. 1st ed. New York: Churchill Livingstone; 1975. pp. 1–20.
[35] Marie NA, Helmy DO, Badawi MA, et al. Image analysis assessment of fibrosis from liver biopsy of chronic hepatitis patients. J Arab Soc Med Res. 2012;7:48–56.
[36] Zeng H, Yuan Z, Zhu H, et al. Expression of Hpnas-4 radiosensitizes Lewis lung cancer. Int J Radiat Oncol Biol Phys. 2012;84:e533–540. doi:10.1016/j.ijrobp.2012.06.028
[37] Samuhasaneeto S, Thong-Ngam D, Kulaputana O, et al. Curcumin decreased oxidative stress, inhibited NF-kappaB activation, and improved liver pathology in ethanol-induced liver injury in rats. J Biomed Biotechnol. 2009;2009:981963. doi:10.1155/2009/981963
[38] Kincaid-Smith J, Tracey A, de Carvalho Augusto R, et al. Morphological and genomic characterisation of the *Schistosoma* hybrid infecting humans in Europe reveals admixture between *Schistosoma haematobium* and *Schistosoma bovis*. PLoS Negl Trop Dis. 2021;15 (12):e0010062. doi: 10.1371/journal.pntd.0010062
[39] Dominici M, Le Blanc K, Mueller I, et al. Minimal criteria for defining multipotent mesenchymal stromal cells. The international society for cellular therapy position statement. Cytotherapy. 2006;8:315–317. doi:10.1080/14653240600855905
[40] Noël D, Caton D, Roche S, et al. Cell specific differences between human adipose-derived and mesenchymal-stromal cells despite similar differentiation potentials. Exp Cell Res. 2008;314(7):1575–1584. doi: 10.1016/j.yexcr.2007.12.022
[41] Lu FB, Chen DZ, Chen L, et al. Attenuation of experimental autoimmune hepatitis in mice with bone mesenchymal stem cell-derived exosomes carrying MicroRNA-223-3p. Mol Cells. 2019;42(12):906–918. doi: 10.14348/molcells.2019.2283
[42] Ko SF, Yip HK, Zhen YY, et al. Adipose-derived mesenchymal stem cell exosomes suppress hepatocellular carcinoma growth in a rat model: apparent diffusion coefficient, Natural killer T-cell responses, and histopathological features. Stem Cells Int. 2015;2015:853506. doi:10.1155/2015/853506
[43] Ohno S, Ishikawa A, Kuroda M. Roles of exosomes and microvesicles in disease pathogenesis. Adv Drug Deliv Rev. 2013;65(3):398–401. doi: 10.1016/j.addr.2012.07.019
[44] Kalluri R. The biology and function of exosomes in cancer. J Clin Invest. 2016;126(4):1208–1215. doi: 10.1172/JCI81135
[45] Frydrychowicz M, Kolecka-Bednarczyk A, Madejczyk M, et al. Exosomes-structure, biogenesis and biological role in nonsmall-cell lung cancer. Scand J Immunol. 2015;81(1):2–10. doi: 10.1111/sji.12247
[46] Harrell CR, Jovicic N, Djonov V, et al. Mesenchymal stem cell-derived exosomes and other extracellular vesicles as new remedies in the therapy of inflammatory diseases. Cells. 2019;8(12):1605. doi: 10.3390/cells8121605
[47] Yang B, Dua W, Wei L, et al. Bone marrow mesenchymal stem cell-derived hepatocyte-like cell exosomes reduce hepatic ischemia/reperfusion injury by enhancing autophagy. Stem Cells Dev. 2020;29(6):372–379. doi: 10.1089/scd.2019.0194
[48] Lr T, Sanchez-Abarca LI, Muntion S, et al. MSC surface markers (CD44, CD73, and CD90) can identify human MSC-derived extracellular vesicles by conventional flow cytometry. Cell Commun Signal. 2016;14(1):2. doi: 10.1186/s12964-015-0124-8
[49] Minor M, Alcedo KP, Battaglia RA, et al. Cell type- and tissue-specific functions of ecto-5'-nucleotidase (CD73). Am J Physiol Cell Physiol. 2019;317 (6):1079–1092. doi: 10.1152/ajpcell.00285.2019
[50] Schneider E, Rissiek A, Winzer R, et al. Generation and function of non-cell-bound CD73 in inflammation. Front Immunol. 2019;10:1729. doi:10.3389/fimmu.2019.01729
[51] Leyton L, Díaz J, Martínez S, et al. Thy-1/CD90 a bidirectional and lateral signaling scaffold. Front Cell Dev Biol. 2019;7:132. doi:10.3389/fcell.2019.00132
[52] Dong L, Pu Y, Chen X, et al. Hucmsc-extracellular vesicles downregulated hepatic stellate cell activation and reduced liver injury in *S. japonicum*-infected mice. Stem Cell Res Ther. 2020;11(1):21. doi: 10.1186/s13287-019-1539-8
[53] Abou Rayia DM, Ashour DS, Abo Safia HS, et al. Human umbilical cord blood mesenchymal stem cells as a potential therapy for schistosomal hepatic fibrosis: an experimental study. Pathog Glob Health. 2022;18:1–13.
[54] Elmalawany AM, Osman GY, Elashwal MS, et al. Protective role of *Balanities aegyptiaca* fruit aqueous extract in mice infected with *Schistosoma mansoni*. Exp Parasitol. 2022;239:108290. doi:10.1016/j.exppara.2022.108290
[55] Ma Z, Liu X, Dong H, et al. Sorafenib and praziquantel synergistically attenuate *Schistosoma japonicum*-induced liver fibrosis in mice. Parasitol Res. 2018;117(9):2831–2839. doi: 10.1007/s00436-018-5972-x
[56] Nono JK, Fu K, Mpotje T, et al. Investigating the antifibrotic effect of the antiparasitic drug Praziquantel in *in vitro* and *in vivo* preclinical models. Sci Rep. 2020;10 (1):1–12. doi: 10.1038/s41598-020-67514-4
[57] Zhang S, Jiang L, Hu H, et al. Pretreatment of exosomes derived from hUcmscs with TNF-α ameliorates acute liver failure by inhibiting the activation of NLRP3 in macrophage. Life Sci. 2020;246:117401. doi:10.1016/j.lfs.2020.117401
[58] Li T, Yan Y, Wang B, et al. Exosomes derived from human umbilical cord mesenchymal stem cells

alleviate liver fibrosis. Stem Cells Dev. 2013;22 (6):845–854. doi: 10.1089/scd.2012.0395
[59] Rong X, Liu J, Yao X, et al. Human bone marrow mesenchymal stem cells-derived exosomes alleviate liver fibrosis through the Wnt/β-catenin pathway. Stem Cell Res Ther. 2019;10(1):98. doi: 10.1186/s13287-019-1204-2
[60] Ohara M, Ohnishi S, Hosono H, et al. Extracellular vesicles from amnion-derived mesenchymal stem cells ameliorate hepatic inflammation and fibrosis in rats. Stem Cells Int. 2018;2018:3212643. doi:10.1155/2018/3212643
[61] Fiore E, Domínguez LM, Bayo J, et al. Human umbilical cord perivascular cells-derived extracellular vesicles mediate the transfer of IGF-I to the liver and ameliorate hepatic fibrogenesis in mice. Gene Ther. 2020;27 (1–2):62–73. doi: 10.1038/s41434-019-0102-7
[62] Shao M, Xu Q, Wu Z, et al. Exosomes derived from human umbilical cord mesenchymal stem cells ameliorate IL-6-induced acute liver injury through miR-455-3p. Stem Cell Res Ther. 2020;11(1):37. doi: 10.1186/s13287-020-1550-0
[63] Alsulami M, Abdel-Gaber R. Cell therapy as a new approach on hepatic fibrosis of murine model of *Schistosoma mansoni*-infection. Acta Parasitol. 2021;66(1):136–145. doi: 10.1007/s11686-020-00267-2
[64] Horton JA, Hudak KE, Chung EJ, et al. Mesenchymal stem cells inhibit cutaneous radiation-induced fibrosis by suppressing chronic inflammation. Stem Cells. 2013;31(10):2231–2241. doi: 10.1002/stem.1483
[65] Santiago E, de Oliveira SA, de Oliveira Filho GB, et al. Evaluation of the anti-*Schistosoma mansoni* activity of thiosemicarbazones and thiazoles. Antimicrob Agents Chemother. 2014;58(1):352–363. doi: 10.1128/AAC.01900-13
[66] Etewa SE, Abd Allah SH, Badawey MSR, et al. The effect of stem cells as an adjuvant on the immunogenicity of a potential anti-schistosomal vaccine in mice. J Egypt Soc Parasitol. 2016;46(3):693–716. doi: 10.12816/0033990
[67] Ibrahim A, Korany H, Hussein T. Pentoxifylline and/or praziquantel reduce murine schistosomiasis mansoni histopathology via amelioration of liver functions. J Aquat Biol Fish. 2019;23(5):121–133. doi: 10.21608/ejabf.2019.67229
[68] Tan CY, Lai RC, Wong W, et al. Mesenchymal stem cell-derived exosomes promote hepatic regeneration in drug-induced liver injury models. Stem Cell Res Ther. 2014;5(3):76. doi: 10.1186/scrt465
[69] Nojima H, Freeman CM, Schuster RM, et al. Hepatocyte exosomes mediate liver repair and regeneration via sphingosine-1-phosphate. J Hepatol. 2016;64 (1):60–68. doi: 10.1016/j.jhep.2015.07.030
[70] Yannaki E, Athanasiou E, Xagorari A, et al. G-CSF–primed hematopoietic stem cells or G-CSF per se accelerate recovery and improve survival after liver injury, predominantly by promoting endogenous repair programs. Exp Hematol. 2005;33(1):108–119. doi: 10.1016/j.exphem.2004.09.005
[71] Ahmed SK, Mohammed SA, Khalaf G, et al. Role of bone marrow mesenchymal stem cells in the treatment of CCL4 induced liver fibrosis in albino rats: A histological and immunohistochemical study. Int J Stem Cells. 2014;7(2):87–97. doi: 10.15283/ijsc.2014.7.2.87
[72] Lan L, Liu R, Qin LY, et al. Transplantation of bone marrow-derived endothelial progenitor cells and hepatocyte stem cells from liver fibrosis rats ameliorates liver fibrosis. World J Gastroenterol. 2018;24 (2):237–247. doi: 10.3748/wjg.v24.i2.237
[73] Almeer RS, El-Khadragy MF, Abdelhabib S, et al. Ziziphus spina-christi leaf extract ameliorates schistosomiasis liver granuloma, fibrosis, and oxidative stress through downregulation of fibrinogenic signaling in mice. PLoS One. 2018;13(10):e0204923. doi: 10.1371/journal.pone.0204923
[74] Shen H, Sheng L, Chen Z, et al. Mouse hepatocyte overexpression of NF-Kb-inducing kinase (NIK) triggers fatal macrophage-dependent liver injury and fibrosis. Hepatology. 2014;60:2065–2076. doi:10.1002/hep.27348
[75] Gong W, Huang F, Sun L, et al. Toll-like receptor-2 regulates macrophage polarization induced by excretory-secretory antigens from *Schistosoma japonicum* eggs and promotes liver pathology in murine schistosomiasis. PLoS Negl Trop Dis. 2018;12(12):e0007000. doi: 10.1371/journal.pntd.0007000
[76] El-Din MI S, El-Hak HN G, Ghobashy MA, et al. Parasitological and histopathological studies to the effect of aqueous extract of Moringa oleifera Lam. leaves combined with praziquantel therapy in modulating the liver and spleen damage induced by *Schistosoma mansoni* to male mice. Environ Sci Pollut Res Int. 2022;28(6):15548–15560. doi: 10.1007/s11356-022-23098-2
[77] Metwally DM, Al-Olayan EM, Alanazi M, et al. Antischistosomal and anti-inflammatory activity of garlic and allicin compared with that of praziquantel *in vivo*. BMC Complement Altern Med. 2018;18(1):135. doi: 10.1186/s12906-018-2191-z
[78] Vannella KM, Wynn TA. Mechanisms of organ injury and repair by macrophages. Annu Rev Physiol. 2017;79 (1):593–617. doi: 10.1146/annurev-physiol-022516-034356
[79] Sen R, Smale ST. Selectivity of the NF-{kappa}B response. Cold Spring Harb Perspect Biol. 2010;2(4):a000257. doi: 10.1101/cshperspect.a000257
[80] Mardpour S, Hassani SN, Mardpour S, et al. Extracellular vesicles derived from human embryonic stem cell-MSCs ameliorate cirrhosis in thioacetamide-induced chronic liver injury. J Cell Physiol. 2018;233(12):9330–9344. doi: 10.1002/jcp.26413